

See discussions, stats, and author profiles for this publication at: <https://www.researchgate.net/publication/4171903>

Detection of visibility conditions through use of onboard cameras

Conference Paper · July 2005

DOI: 10.1109/IVS.2005.1505101 · Source: IEEE Xplore

CITATIONS

9

READS

59

3 authors, including:



Nicolas Hautière

Institut Français des Sciences et Technolog...

96 PUBLICATIONS 998 CITATIONS

SEE PROFILE



Raphael Labayrade

Ecole Nationale des Travaux Publics de l'Etat

73 PUBLICATIONS 1,062 CITATIONS

SEE PROFILE

Detection of Visibility Conditions through use of Onboard Cameras

Nicolas HAUTIERE, Raphaël LABAYRADE and Didier AUBERT

LIVIC - INRETS / LCPC, building 824, 14 route de la Minière

78000 Versailles Satory, France

nicolas.hautiere@lcpc.fr, raphael.labayrade@lcpc.fr, didier.aubert@inrets.fr

Abstract—An atmospheric visibility measurement system capable of quantifying the most common operating range of onboard exteroceptive sensors is a key parameter in the creation of driving assistance systems. This information is then utilized to adapt sensor operations and processing or to alert the driver that the onboard assistance system is momentarily inoperative. Moreover, a system capable of either detecting the presence of fog or estimating visibility distances constitutes in itself a driving assistance. In this paper, we present a measurement framework of different visibility distances using onboard CCD cameras, that we beforehand defined: meteorological visibility, obstacle visibility, mobilized visibility. The methods to estimate these different visibility distances are detailed. Whereas the first one is based on a physical model of light diffusion by the atmosphere, the two other methods are based on the "v-disparity" approach and local contrasts computation. The methods are evaluated thanks to video sequences under sunny weather and foggy weather.

I. INTRODUCTION

Perception sensors (cameras, laser, radar...) are being introduced into certain vehicles. These sensors have been designed to operate within a wide range of situations and conditions (weather, luminosity, etc.) with a prescribed set of variation thresholds. Effectively detecting when a given operating threshold has been surpassed constitutes a key parameter in the creation of driving assistance systems that meet required reliability levels. With this context in mind, an atmospheric visibility measurement system may be capable of quantifying the most common operating range of onboard exteroceptive sensors. This information is then utilized to adapt sensor operations and processings or to alert the driver that the onboard assistance system is momentarily inoperative. Moreover, a system capable of either detecting the presence of fog or estimating visibility distances constitutes in itself a driving assistance. Indeed, during foggy weather, humans actually tend to overestimate visibility distances [2], which can lead to excessive driving speeds. Nevertheless, this topic has been hardly tackled in the literature. Only Pomerleau [10] estimated visibility by means of measuring the contrast attenuation of road markings at various distances in front of a moving vehicle. This approach, based on the "RALPH" system, nonetheless requires the presence and detection of road markings in order to proceed.

Koschmieder's law models the fog effects on atmospheric visibility. One of its parameters is the extinction coefficient of fog k . This parameter is strongly linked to the meteorological visibility proposed by the International Commission on

Illumination [1]. So, we tried to develop a method estimating k . This technique is summarized in the section II. In order to cover more situations than solely daylight foggy weather, we developed a more generic approach. Thus, we estimate the distance to the most distant object having enough contrast and belonging to the surface of the road. We called this distance the mobilized visibility distance. We will see that this distance is very close to the definition of the meteorological visibility. The method is presented in the section III. Finally, in section IV, we present our measurement framework based on stereovision, which estimates at the same time the different visibility distances and is also able to detect road obstacles thanks to the "v-disparity" approach [7].

II. KOSCHMIEDER'S MODEL AND METEOROLOGICAL VISIBILITY

In this section, we present Koschmieder's model, on which part of our work is based. We define the meteorological visibility distance. Then, the method to estimate this distance is briefly presented.

A. Koschmieder's Model

In 1924, Koschmieder [8] proposes his theory on the apparent luminance of objects observed against background sky on the horizon. In noting that a distant object winds up blending in with the sky, he establishes a simple relationship between the distance d of an object with intrinsic luminance L_o and its apparent luminance L as follows:

$$L = L_o e^{-kd} + L_f (1 - e^{-kd}) \quad (1)$$

where L_f denotes the luminance of the sky and k the extinction coefficient of the atmosphere.

Based on these results, Duntley [8] derives an attenuation law of atmospheric contrasts:

$$C = C_o e^{-kd} \quad (2)$$

where C designates the apparent contrast at distance d and C_o the intrinsic contrast of the object against its background.

This law is only applicable in the case of uniform illumination of the atmosphere. In order for the object to be just barely visible, the value of C must equal the contrast threshold ε . From a practical standpoint, the CIE [1] has adopted an average value of $\varepsilon = 0.05$ for the contrast threshold so as

to define a conventional distance, called the "meteorological visibility distance" V_{met} , i.e. the greatest distance at which a black object ($C_o = 1$) of a suitable dimension can be seen in the sky on the horizon.

$$V_{met} = -\frac{1}{k} \ln(0.05) \simeq \frac{3}{k} \quad (3)$$

B. Estimation of the Meteorological Visibility

In [3], we succeed to instantiate Koschmieder's model and then to estimate the meteorological visibility distance under daytime foggy weather. For this purpose, we measure the intensity variation of the road vertically in the image and we search the position of an inflection point on this curve. The value of k is then expressed as follows :

$$k = \frac{2(v_i - v_h)}{\lambda} \quad (4)$$

where v_i is the position of the inflection point, v_h the position of the horizon line and λ depends on the intrinsic and extrinsic parameters of the camera. v_h can be estimated by intersecting vanishing lines [11]. Using a stereo sensor and the "v-disparity" approach, the position of the horizon line and consequently the pitch angle of the camera can be computed dynamically [7]. One advantage of this method is that we only need one camera and the presence of the road and the sky in the image. The latter are detected thanks to a region growing process, which is used to detect the fog presence (cf. Fig. 8i). If there is no fog, i.e. the region growing does not cross the image from bottom to top, our method is also able to detect it like on Fig. 1a. This is very useful and important to create a reliable driving assistance.



Fig. 1. Results of fog detection and measurement of the meteorological visibility distance; (a) under sunny weather, the region growing does not cross the image from bottom to top. Consequently, the method indicates that there is no fog on the picture using a small triangle; (b) under foggy weather, the method detects fog. The curve on the left represents the luminance variation measured between the right and left borders painted black on the figure. The visibility distance is represented by an horizontal black line.

III. MEASUREMENT OF THE MOBILIZED VISIBILITY DISTANCE

In this section, we estimate the "mobilized visibility distance", which is the distance to the most distant object having enough contrast and belonging to the surface of the road. This definition is close to the definition of the meteorological visibility. The link between these two distances is the topic of the first paragraph. Then, to estimate this "mobilized visibility

distance", we must achieve two different tasks. We have to compute a depth map of the environment ahead of the vehicle. This is the topic of the paragraph III-B. Moreover, we detect obstacles which occlude part of the road and the traffic. Then, we have to compute the contrasts above a certain threshold in the image. The threshold to consider is discussed. Finally, we have to combine the depth map and the selected contrasts.

A. Definition of New Visibility Distances

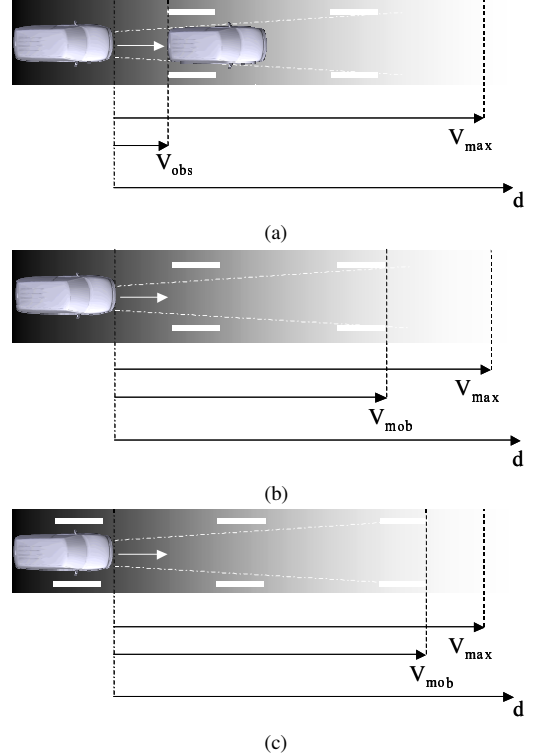


Fig. 2. Examples of (a) obstacle V_{obs} , (b) mobilized V_{mob} and (c) mobilizable V_{max} distances of visibility.

On Fig. 2, we represent a simplified road with dash road marking and at least one vehicle moving on it. The first visibility distance is obstacle visibility V_{obs} . Indeed, an obstacle which is big enough to mask the field of view prevents the driving entity to see its trajectory. This is the case on Fig. 2a. If there is no obstacles, we can see from the Fig. 2b that the most distant visible object is the extremity of the last road marking. However, the extremity location depends on the vehicle position, like on Fig. 2c. We call this distance, which depends on the road scene, the mobilized visibility distance V_{mob} . This distance ought to be compared to the "mobilizable visibility distance" V_{max} , which is the greatest distance at which a potential object on the road surface would be visible.

The mobilizable visibility distance can be expressed as a function of the meteorological visibility distance defined by the CIE [1] and the contrast threshold \tilde{C}_{BW} between a "black" object and a "white" object. We denote L_{b_0} and L_{w_0} , the intrinsic luminances and L_b et L_w the luminances at the

distance d of the "black" object B and the "white" object W .

Koschmieder's law gives us the theoretical variations of this values according to the distance d . Let's express the contrast C_{BW} of W with respect to B :

$$C_{BW} = \frac{\Delta L}{L} = \frac{(L_{w0} - L_{b0})e^{-kd}}{L_{b0}e^{-kd} + L_f(1 - e^{-kd})} \quad (5)$$

We deduce the expression of d according to the photometric parameters, the contrast C_{BW} and the meteorological visibility distance V_{met} :

$$d = -\frac{V_{met}}{3} \ln \left(\frac{C_{BW}L_f}{L_{w0} - L_{b0} + C_{BW}(L_f - L_{b0})} \right) \quad (6)$$

It is the distance to which an object W is perceived with a contrast of C_{BW} . Like CIE does, we can choose a threshold \tilde{C}_{BW} below which the object is considered as being not visible. Like for the computation of the meteorological visibility distance, we assume that the intrinsic road luminance is equal to zero. Thus, after maximisation, we obtain the value of V_{max} :

$$V_{max} = -\frac{V_{met}}{3} \ln \left(\frac{\tilde{C}_{BW}}{1 + \tilde{C}_{BW}} \right) \quad (7)$$

We obtain easily the value \tilde{C}_{BW} so that $V_{max} = V_{met}$:

$$\tilde{C}_{BW} = \frac{1}{e^3 - 1} \approx 5 \% \quad (8)$$

Consequently, by choosing a threshold of 5 %, the mobilizable distance of visibility is very close to the meteorological visibility distance, that we are able to compute under daytime foggy weather (cf. section II). These definitions lead to the following relationship:

$$V_{obs} < V_{mob} \leq V_{max} \approx V_{met} \quad (9)$$

B. Computation of a Depth Map of the Environment by Stereovision

In this section, we introduce our stereoscopic sensor. Then, we present our technique to detect obstacles and compute a depth map of the environment using the "v-disparity" approach. The various computation stages are detailed.

1) *Modeling of the Stereo Sensor*: The two image planes of the stereo sensor are supposed to belong merely to the same plane and are at the same height above the road (see Fig. 3). This camera geometry means that the epipolar lines are parallel.

2) *The image of a plane in the "v-disparity" image*: In this study, we segment the environment into planes which are horizontal, vertical or oblique with respect to the plane of the stereoscopic sensor. In a cross-section of the scene in the optical axis of the camera, the projection of any of these planes is a straight line. In the remaining of this paper, we will build and use a specific image in which the detection

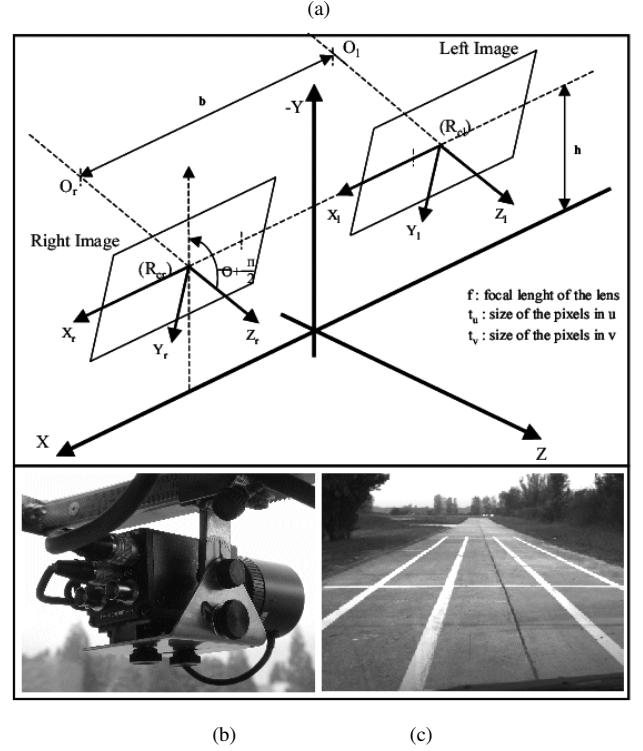


Fig. 3. (a) The stereo sensor and the coordinate systems used. (b) Cameras currently in use in the prototype cars of the LIVIC. (c) Calibration site on the test track of Versailles Satory.

of straight lines will be equivalent to the detection of planes in the scene. Indeed, we will represent the v coordinate of a pixel towards the disparity Δ and detect straight lines and curves in this 2D image. Mathematical framework is given in [7].

3) *"V-Disparity" Image Construction and Obstacle Detection*: To compute a disparity map I_{Δ} , the primitives used are horizontal local maxima of the gradient. The matching process is quite simple and fast. It is based on normalized correlation around the local maxima. Once I_{Δ} has been computed, the "v-disparity" image $I_{v\Delta}$ is built by accumulating the pixels of same disparity in I_{Δ} along the \vec{v} axis. Then straight lines are detected in $I_{v\Delta}$ thanks to a hough transform. This leads to extract global surfaces, which correspond either to the road surface, or to obstacles. Details of this method are given in [7] and an example of "v-disparity" image is given on Fig. 8f.

4) *Disparity Map Improvement*: In order to quickly compute the "v-disparity" image, a sparse and rough disparity map has been built (cf. Fig. 8c). This disparity map may contain numerous false matches, which prevents us to use it as a depth map of the environment. Thanks to the global surfaces extracted from the "v-disparity" image, false matches can be removed. In this aim, we check whether a pixel of the disparity map belongs to any global surface extracted using the same

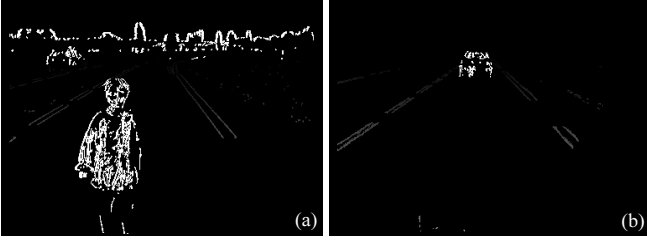


Fig. 4. Examples of disparity map of the vehicle environment (a) under sunny weather, (b) under foggy weather. White points are considered as obstacles points. The gray level of other points is proportional to their disparity.

matching process. If it the case, the disparity value is mapped to the pixel. Details of this process can be found in [6]. Finally, this enhanced disparity can be used as a depth map of the environment ahead of the vehicle. Some examples of improved disparity maps are shown on Fig. 4.

C. Computation of Contrasts above 5 %

Local contrasts computation has only received minimal attention in the literature. We developed a technique using sliding windows, inspired from Köhler's binarization technique [5], which goes quite fast and is robust to noise. The original technique finds the threshold which maximizes the mean contrast $C(s_0)$ between two parts of the image along the associate border $F(s_0)$ for a given definition of local contrast C_{x,x_1} between two pixels x and x_1 .

$$C(s_0) = \max_{s \in [0, 255]} \frac{1}{\text{card}(F(s))} \sum_{(x, x_1) \in F(s)} C_{x, x_1}(s) \quad (10)$$

We chose to estimate the logarithmic contrast [4] defined by (11), so as to be in accordance with the definition of the meteorological visibility distance:

$$C_{x, x_1}(s) = \min \left(\frac{|s - x|}{\max(s, x)}, \frac{|s - x_1|}{\max(s, x_1)} \right) \quad (11)$$

Finally, the evaluated contrast is equal to $2C(s_0)$ along the associated border $F(s_0)$. Some examples of local contrasts computations are shown on Fig. 5.

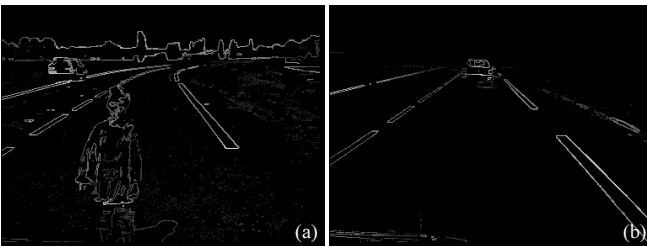


Fig. 5. Examples of contrasts computation above 5 % on the whole images, (a) under sunny weather, (b) under foggy weather.

D. Fast Disparity-Contrast Combination

Once the improved disparity map is achieved, we scan it starting from the horizon line. Indeed, most distant objects on the road surface are on the horizon line. The contrast is calculated within each neighborhood which contains no obstacle points and where the disparity of a pixel is known. The process stops when a contrast above 5 % is met. The visibility distance V_{mob} is then the distance associated with the disparity Δ of the pixel with a contrast above 5 %. The algorithm is summarized on Fig. 6 and some final results are given on Fig. 7.

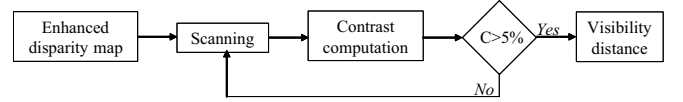


Fig. 6. Algorithm overview

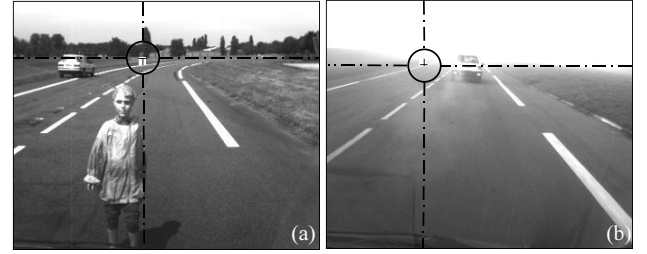


Fig. 7. Final result: the most distant window having a contrast above 5 %, on which a point of disparity is known, is painted white. The known disparity point is represented with a black cross on the white window. (a) sunny weather ($V_{mob} \approx 250m$), (b) foggy weather ($V_{mob} \approx 75m$).

IV. IMPLEMENTATION AND EVALUATION OF THE METHODS

A. Experimental Platform

The different methods have been tested on our experimental prototypes. The whole process is performed within 100 ms with a current-day PC. The hardware used for the experiments is an Intel Pentium IV 2.4 GHz. Images are grabbed using a Matrox Meteor II graphic card. The focal length is 8.5 mm. Image size is 380x289. The program runs on the RT-Maps platform [9] and is compiled with the Intel C++ Compiler 8.0. The Fig. 8 presents an overview of the image processing framework.

B. Test video sequences

This method has been tested on two video sequences, each containing over 1000 images. In the first sequence, the instrumented vehicle is following another car at various distances and stops in front of different obstacles. The weather is sunny and clear. In the second sequence, the instrumented vehicle is following another car, which disappears progressively through the thick fog. Both sequences take place on a part of the test track of Versailles Satory. A sample of each sequence is used to illustrate the methods.

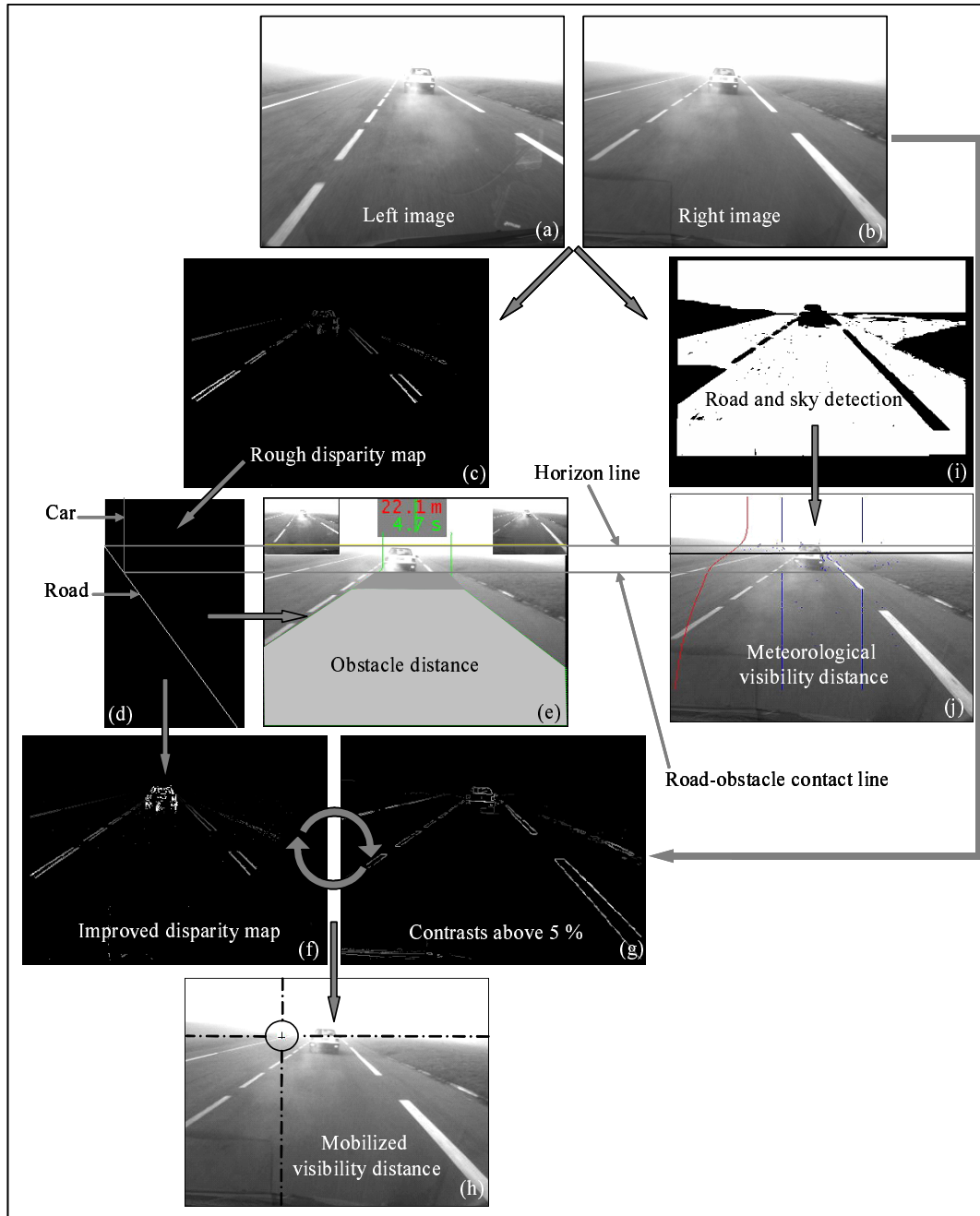


Fig. 8. Visibility distance measurement framework. (a) Left original image; (b) right original image; (c) rough disparity map computed from images (a) and (b); (d) extracted lines from the "v-disparity" image; (e) road-obstacle contact line and time to collision measurement; (f) obstacle areas (in white) and disparity values (in gray levels) on the road surface; (g) contrast above 5 % computed on the whole image; in the algorithm, the contrast is computed in only few windows; (h) the most distant window having a contrast above 5 %, on which the disparity of a pixel is known, is painted white. The known disparity point is represented with a black cross on the white window; (i) region growing process detecting picture elements compatible with the Koschmieder model; (j) measurement of the meteorological visibility distance represented by a horizontal black line.

C. Results

On Fig. 1 and Fig. 8i, the results of fog detection and measurement of the meteorological visibility distance are represented. On Fig. 1a, the method does not detect fog and says it using a small triangle. Conversely, on Fig. 1b and Fig. 8j, the method detects fog. The visibility distance is

represented by a horizontal black line. We also represented the curve of the luminance variation measured on each line of a bandwidth, which borders are represented vertically on the picture. As we can see, this bandwidth is able to get round the obstacle to take into account only the road and the sky.

On Fig. 4 and Fig. 8f, the results of disparity map computa-

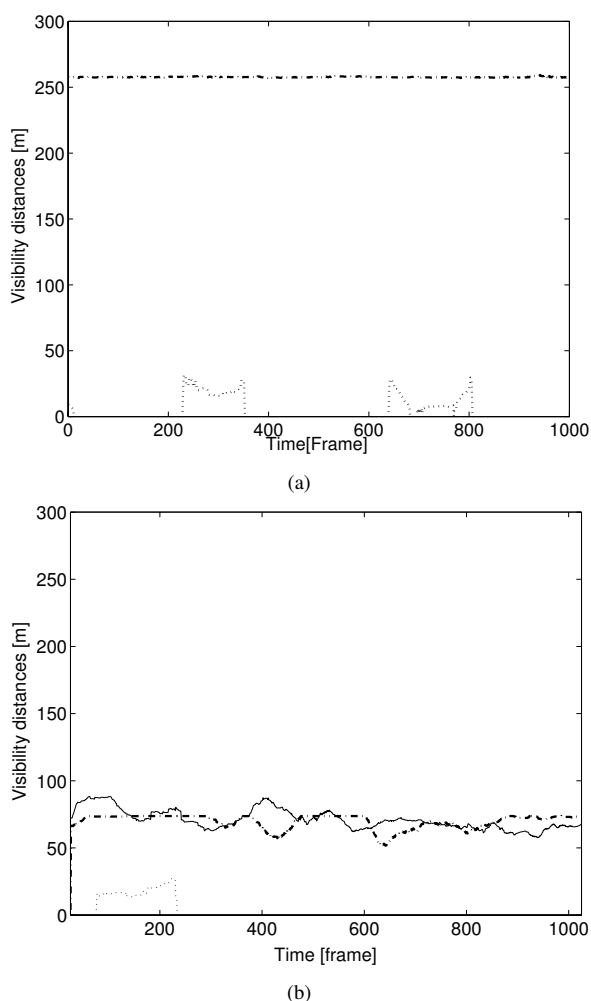


Fig. 9. curves of measures: (---) mobilized distance of visibility, (—) meteorological visibility distance, (...) obstacle distance of visibility (a) under sunny weather; (b) under foggy weather.

tions are presented. On Fig. 4a, the pedestrian, the car, points beyond horizon line are considered as obstacles points. The disparity of the points on the road surface is computed. In the same way, on Fig. 4b and Fig. 8f, the car is considered as an obstacle. On the latter, far less disparity points are known because of the reduced visibility.

On Fig. 5 and Fig. 8g, the results of local contrast computation on the whole images are represented. In fact, as explained in section III-D, the contrast is not computed on the whole image to save computing time. On Fig. 7 and Fig. 8h, the final result is represented. The most distant window having a contrast above 5 %, on which the disparity of a pixel is known, is painted white. This pixel is represented with a black cross inside the white window.

On Fig. 9, the curves of measured visibility distances are plotted. On Fig. 9a, under sunny weather, the mobilized visibility distance is equal to the maximum detection range of the sensor. Conversely, under foggy weather, on Fig. 9b, the mobilized visibility distance is strongly reduced due to

the presence of fog. This curve is very similar to the one of the meteorological visibility distance, what is not surprising. Finally, we also plotted the curves of obstacle visibility distance.

V. CONCLUSION

In this paper, we presented an image processing framework able to measure different visibility distances, including obstacle detection and fog detection. Obstacle detection is made using the "v-disparity" approach. Thanks to an instantiation of Koschmieder's model, we are able to detect fog and to estimate the meteorological visibility distance. What we called mobilized visibility distance is estimated using a combination of an original local contrast computation and an improved disparity map. The whole process is performed within 100 ms using a Pentium IV 2.4 GHz. Finally, we evaluated the methods with two different video sequences of 1000 images each under sunny and foggy weather. Other environmental conditions (rain, snowstorm, sandstorm...) are taken into account, insofar as the contrast in the road scene is impaired in these situations. On the other hand, estimating their effects on the windshield is not considered. Finally, in order to evaluate the performance of our methods and to calibrate them, we are currently building targets on the test track of Versailles Satory so as to provide a reference measure of the atmospheric diffusion. To be able to give a probabilistic output of the certainty of the measurements is also an interesting prospect.

ACKNOWLEDGMENTS

The authors would like to acknowledge the contribution of Éric Dumont, researcher at LCPC and Michel Jourlin, Professor at the University of Saint-Étienne. This work is partly founded by the French ARCOS project.

REFERENCES

- [1] *International lighting vocabulary*. Commission Internationale de l'Éclairage, 1987, no. 17.4.
- [2] V. Cavallo, M. Colomb, and J. Doré, "Distance perception of vehicle rear lights in fog," *Human Factors*, vol. 43, pp. 442–451, 2001.
- [3] N. Hautière and D. Aubert, "Driving assistance: automatic fog detection and measure of the visibility distance," in *ITS World Madrid*, November 2003.
- [4] M. Jourlin and J.-C. Pinoli, "Logarithmic image processing," *Advances In Imaging and Electron Physics*, vol. 115, pp. 129–196, 2001.
- [5] R. Köhler, "A segmentation system based on thresholding," *Graphical Models and Image Processing*, vol. 15, pp. 319–338, 1981.
- [6] R. Labayrade and D. Aubert, "In-vehicle obstacles detection and characterization by stereovision," in *IEEE ICVS Graz Austria*, November 2003.
- [7] R. Labayrade, D. Aubert, and J.-P. Tarel, "Real time obstacle detection in stereovision on non flat road geometry through v-disparity representation," in *IEEE Transactions On Intelligent Vehicles*, 2002.
- [8] W. Middleton, *Vision through the atmosphere*. University of Toronto Press, 1952.
- [9] F. Nashashibi, B. Steux, P. Coulombeau, and C. Laugeau, "Rt-maps a framework for prototyping automotive multi-sensor applications," in *IEEE Intelligent Vehicles Symposium, Dearborn, MI, USA*, October 2000.
- [10] D. Pomerleau, "Visibility estimation from a moving vehicle using the ralph vision system," in *IEEE Conference on Intelligent Transportation Systems*, November 1997, pp. 906–911.
- [11] J.-P. Tarel, D. Aubert, and F. Guichard, "Tracking occluded lane-markings for lateral vehicle guidance," in *IEEE CSCC'99*, 1999.